

# ENSEMBLE CAVITY CONTROL SYSTEM SIMULATION USING PULSE-TO-PULSE CALIBRATION

C. Serrano, L. Doolittle, A. Ratti, A. Vaccaro, LBNL, Berkeley, CA 94710, USA

## Abstract

For cost reasons one klystron will supply RF power to multiple cavities in recent projects. Individual cavity field stability and optimal drive needs to be achieved considering beam propagation, cavity tuning, cavity coupling, and cable lengths. External environmental factors continuously modify physical properties of the accelerating structures and waveguides. Therefore a calibration system has been designed to adapt individual drive signals and vector-sum alignment in a pulse-to-pulse basis. An eight-cavity model and a calibration system have been tested in simulation using the hardware-software simulation tool developed at LBNL [1].

## INTRODUCTION

When multiple cavities are powered by a single external RF source, control is applied to the vector sum of the cavity fields. Thus, the controlled variable is the RF field seen by the beam, as if it were passing through a single accelerating structure. Each measured cavity field needs thus to represent its contribution to the overall accelerating field.

Proper operation of applications-level software is essential for the cavities to accelerate the beam. It is used to accurately set several parameters per cavity, based on complex math and live data collected from the front end, including interaction with the real-time digital logic coded into a Field Programmable Gate Array (FPGA). Finally, there is extraordinary financial and schedule motivation to make this software work the first time: debugging on a live accelerator is expensive and potentially dangerous.

The process described in this paper has led to a code base that works in a relatively complete simulated environment. This is necessary, although perhaps not sufficient, for the final hardware/software system to work correctly with actual beam.

## LLRF CONTROL SYSTEM

In modern systems, feedback control is performed digitally using FPGAs. Their increased density allow us to include in their functionality other operations such as vector alignment, sum calculation, and communication with software devices. The system is then centered around an FPGA. It receives the measured cavity fields and drive signals, after analog-to-digital conversion. The FPGA operates in IQ representation at baseband or at an intermediate frequency. Digital frequency conversion and IQ (de)modulation is also performed in the FPGA.

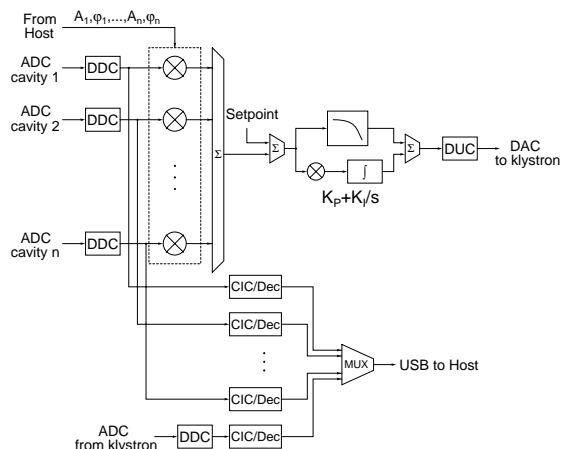


Figure 1: Simplified block diagram the LLRF control system implemented in an FPGA

A rotation matrix is applied to each cavity field for vector sum alignment (both amplitude and phase), and the result of the vector sum is inserted into a Proportional and Integral (PI) controller. The controlled signal is then sent to the klystron after digital-to-analog conversion.

In parallel, the cavity-field and drive signals, are CIC (Cascaded Integrator-Comb) filtered in decimation mode, and sent to a host computer for calibration parameter computation. These parameters include amplitude and phase compensation for vector sum alignment, and phase compensation for the PI controller.

## MODEL

In order to test the functionality of the FPGA and the host computer, an RF model has been implemented in software to calculate the system response after one simulation step. The RF model includes the klystron, the cavities (including detuning), analog filters, and the beam as it propagates from one cavity to the other.

The propagation of signals through different waveguides is represented by phase rotations and attenuations, and individual noise sources have been inserted for each measured signal. Fig. 2 shows a simplified block diagram of the model used for simulation tests.

Finally, the synthesizable hardware design, the host computer, the RF model, and their interactions are simulated in an all-digital, virtualized-time simulation environment [1].

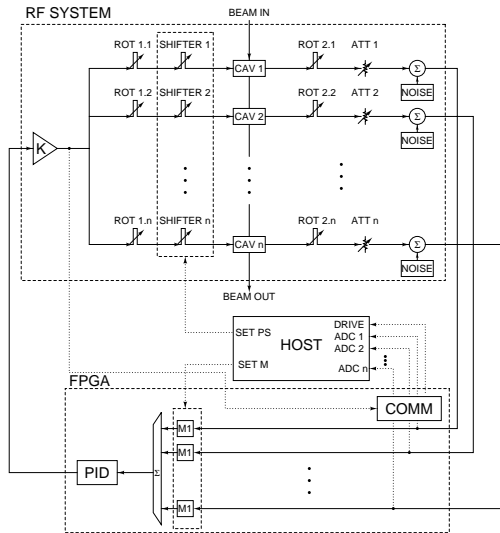


Figure 2: Block diagram of the ensemble cavity control system model

## PHYSICS

There are several sources of misalignment affecting both the vector sum of the cavity fields, and the high power signal driving each cavity. In this section we define the differential equation describing the modulated cavity field vector (available in the FPGA), we determine which are the sources of misalignment, and we analyze their effects on the system.

### Description of the Modulated Cavity Field Vector

RF cavities can be considered as an RLC parallel circuit [2], being excited at a frequency close to resonance. Reporting this to baseband and sampling at  $90^\circ$ , makes the transfer function become a first-order low-pass filter for both I and Q components, with a small offset from DC. Thus, we can consider the cavity field impulse response as a decaying exponential modulating an oscillating term representing detuning, with two coupled generators: the klystron, and the beam. The RF field in the  $i^{th}$  cavity is then expressed as:

$$\frac{dE_i}{dt} + c \cdot E_i = a \cdot K + b \cdot I_i \quad (1)$$

where  $E_i$  and  $I_i$  are the cavity field and the beam current in the  $i^{th}$  cavity respectively, and  $K$  is the common drive signal. The cavity fields and drive are measured, and the beam current is considered to be well known. We know the differential equation of the cavity field as a function of the two coupled generators, as it is inside the cavity.  $a$ ,  $b$ , and  $c$  are unknown complex numbers:  $a$  and  $b$  report that differential equation onto the FPGA level, as a result of the cavity field measuring operation, and  $c$  represents cavity rise time and detuning.

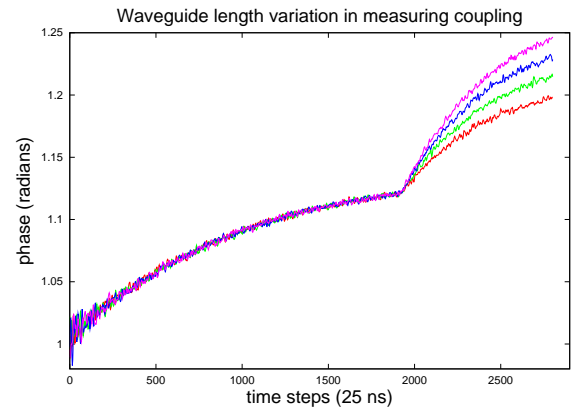


Figure 3: Cavity phase variation at beam loading due to waveguide length variation in the measuring coupling

### Sources of Vector Misalignment

Each of the unknown complex numbers in eq. 1 give us information about the different sources of misalignment in the system: propagation through waveguides in both the power and measuring couplings, and cavity detuning. Cavity detuning can be found by determining the imaginary component of  $c$  in eq. 1 for each cavity. Then, we need to differentiate the effects of the propagation through waveguides in both couplings.

It can be observed in fig. 2 that the cavity induced field by the high-power source travels through both couplings, whereas the beam induced beam only travels through the measuring coupling. Therefore  $a$  and  $b$  in eq. 1 contain information about the total propagation effect, and that occurring only in the measuring coupling, respectively.

Fig. 3 illustrates how the difference between the phase shifts in both couplings is found. For illustrative purposes, the phase of the RF field in four cavities is represented, where the phase shift due to propagation in the measuring coupling has been increased by 0.2 radians from one cavity to the other. The phase shift in the power coupling has been set so that the total phase shift is identical in every line. We then observe that the cavity phase is identical in all cases until the beam loading occurs (at time step 1900), where the beam induced field polarity varies according to the phase shift variation in the measuring coupling.

## CALIBRATION SYSTEM

The calibration system is run in a host computer, which receives the cavity fields and drive waveforms from the FPGA. These waveforms are curve fitted according to eq. 1 in order to find the complex unknown numbers:  $a$ ,  $b$ , and  $c$ . From these, the calibration parameters are deduced, and sent to the FPGA in a pulse-to-pulse basis.

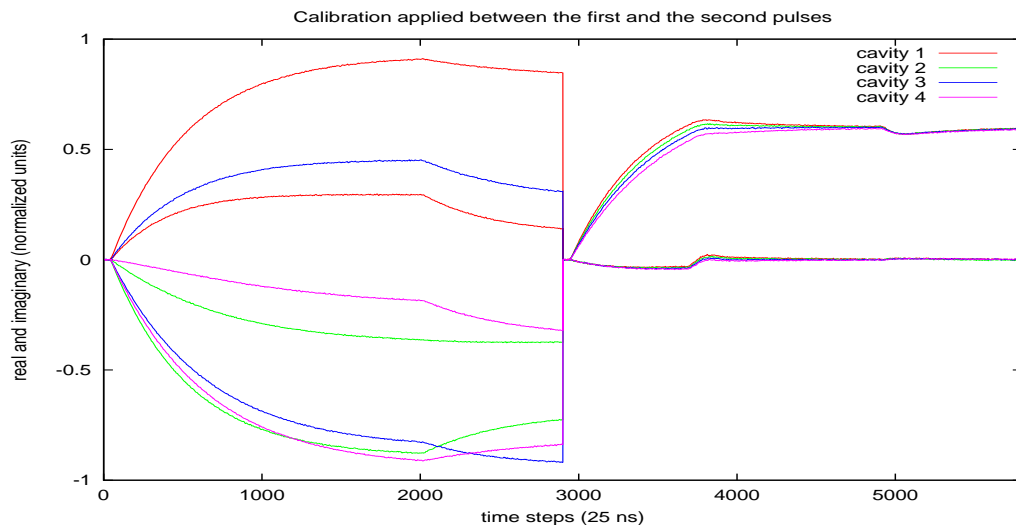


Figure 4: RF field in four cavities with different Q during two  $72.5 \mu s$  pulses. Waveforms are measured during a first open-loop pulse, where the phase shifts in both couplings are initialized to a random value between 0 and  $2\pi$ , and the attenuation between 0 and 0.3% of the nominal cavity field. Calibration is applied between the first and the second pulses.

### Curve Fitting Algorithm

Eq. 1 can be expressed in discrete form as:

$$D_i[n] = a \cdot K[n] + b \cdot I_i[n] - c \cdot E_i[n] \quad (2)$$

where  $D_i$  is the discrete derivative of the  $i^{th}$  cavity field. Given N data points obtained from waveform measurement during one pulse, eq. 2 can be expressed in matrix form as:

$$\begin{pmatrix} D_i[1] \\ D_i[2] \\ \vdots \\ D_i[N] \end{pmatrix} = \begin{pmatrix} K[1] & I_i[1] & -E_i[1] \\ K[2] & I_i[2] & -E_i[2] \\ \vdots & \vdots & \vdots \\ K[N] & I_i[N] & -E_i[N] \end{pmatrix} \times \begin{pmatrix} a \\ b \\ c \end{pmatrix}$$

We then obtain a  $N \times 3$  equation system to solve for  $a$ ,  $b$ , and  $c$ , which can be found by traditional matrix techniques [3]. Since the beam is not present during the cavity build-up period, the process can be further simplified by decomposing the solution into two curve fittings: find  $a$  and  $c$  during the build-up period (where  $I_i=0$ ), then find  $b$  during cavity beam loading. A single three-parameter fit thus reduces to a two-parameter least-squares fit followed by a one-parameter fit (simple average).

### Calibration Results

The phase of the common drive signal is measured, and the effect of waveform propagation in each power coupling is deduced by curve fitting. Thus, in the case of having fast phase shifters in the high power section, we can establish each cavity field phase relative to the beam according to the accelerator specs, by applying the necessary compensation.

Cavity detuning and the effect of propagation through waveguides in the measuring coupling have been deduced. A rotation matrix is applied before calculating the

vector-sum, compensating for phase shift in the measuring coupling, relative attenuation levels, as well as different detuning levels.

Fig. 4 shows the real and imaginary components of the RF field in four cavities, during two  $72.5 \mu s$  pulses. The first pulse has randomly set physical properties, no software correction, and intra-pulse feedback disabled.

Based on the data collected during that first pulse, calibration is applied, and the resulting aligned cavity fields are observed in the second pulse. The time elapsed between pulses is generally much longer than the pulse length, and has been omitted for illustration purposes. This operation is repeated every pulse, so long-term drifts in waveguide properties and detuning can also be compensated.

## CONCLUSIONS

An ensemble cavity control system using pulse-to-pulse calibration has been modeled and simulated, proving good response to known perturbations. The functionality of the FPGA, the calibration system, and their interactions, has been validated using a HW/SW simulation tool [1].

## REFERENCES

- [1] A. Vaccaro, L. Doolittle, A. Ratti, C. Serrano, "Hardware-Software Simulation for LLRF control system development," EPAC'08, June 2008, Genoa, <http://www.JACoW.org>
- [2] Thomas P. Wangler, "RF Linear accelerators," Wiley-Interscience, 1998
- [3] W. H. Press, S. A. Teukolsky, W. T. Vetterling, B. P. Flannery, "Numerical Recipes in C, The Art of Scientific Computing," Cambridge University Press, 2nd edition, 1992